

# A self calibrating, magnetic sensor approach accurately positions an aortic damage control stent in a porcine model

Dahlia M Kenawy <sup>1</sup>, Yifan Zhang,<sup>2</sup> Moataz Elsisy,<sup>2,3</sup> Mahmoud Abdel-Rasoul,<sup>4</sup> Youngjae Chun,<sup>2</sup> William C Clark,<sup>2</sup> Bryan W Tillman <sup>1</sup>

<sup>1</sup>Surgery, The Ohio State University Wexner Medical Center, Columbus, Ohio, USA

<sup>2</sup>Swanson School of Engineering, University of Pittsburgh, Pittsburgh, Pennsylvania, USA

<sup>3</sup>Mechanical Design and Production Department, Cairo University Faculty of Engineering, Cairo, Egypt  
<sup>4</sup>Biomedical Informatics, The Ohio State University Wexner Medical Center, Columbus, Ohio, USA

## Correspondence to

Dr Bryan W Tillman; bryan.tillman@osumc.edu

This work was presented at the American College of Surgeons Clinical Congress 2022 in San Diego, California, USA from October 16–20, 2022.

Received 23 July 2023

Accepted 9 October 2023

## ABSTRACT

**Objectives** Non-compressible torso hemorrhage remains a high mortality injury, with difficulty mobilizing resources before exsanguination. Previous studies reported on a retrievable stent graft for damage control and morphometric algorithms for rapid placement, yet fluoroscopy is impractical for the austere environment. We hypothesized that magnetic sensors could be used to position stents relative to an external magnet placed on an anatomic landmark, whereas an electromagnet would allow self-calibration to account for environmental noise.

**Methods** A magnetic sensor alone (MSA) and with integrated stent (MSIS) were examined in a porcine model under anesthesia. A target electromagnet was placed on the xiphoid process (position 0 cm). Sensors were placed in the aorta and measurements obtained at positions 0 cm, +4 cm, and +12 cm from the magnet and compared with fluoroscopy. Sensors were examined under conditions of tachycardia/hypertension, hypotension, vibration, and metal shrapnel to simulate environmental factors that might impact accuracy. General linear models compared mean differences between fluoroscopy and sensor readings.

**Results** Both sensors were compatible with a 10 French catheter system and provided real-time assessment of the distance between the sensor and magnetic target in centimeters. Mean differences between fluoroscopy and both magnetic sensor readings demonstrated accuracy within  $\pm 0.5$  cm for all but one condition at 0 cm and +4 cm, whereas accuracy decreased at +12 cm from the target. Using the control as a reference, there was no significant difference in mean differences between fluoroscopy and both MSA or MSIS readings at 0 cm and +4 cm for all conditions. The system retained effectiveness if the target was overshoot.

**Conclusion** Magnetic sensors achieved the highest accuracy as sensors approached the target. Oscillation of the electromagnet on and off effectively accounts for environmental noise.

This approach is promising for rapid and accurate placement of damage control retrievable stent grafts when fluoroscopy is impractical.

**Level of evidence** Not applicable.

## BACKGROUND

Despite advances in trauma surgery during the past few decades, non-compressible torso hemorrhage (NCTH) remains a significant challenge, with mortality rates of up to 70% in civilian and military trauma patients.<sup>1</sup> Major open abdominal surgery

## WHAT IS ALREADY KNOWN ON THIS TOPIC

- ⇒ Non-compressible torso hemorrhage is a high mortality injury, with few options available to stabilize patients in emergent settings.
- ⇒ Endovascular technology offers the ability to provide hemorrhage control from aortic injuries, particularly retrievable stent grafts, which are currently only in experimental use.
- ⇒ However, standard of care dictates fluoroscopic placement of these devices, a technique which is prohibitive in emergent and austere settings.
- ⇒ A portable solution to allow placement of endovascular devices efficiently and accurately is an important component in addressing this clinical problem.

## WHAT THIS STUDY ADDS

- ⇒ This is the first study to demonstrate the use of an electromagnet for accurate placement of endovascular devices under different physiologic and environmental conditions that may be experienced with patients presenting with non-compressible torso hemorrhage.

## HOW THIS STUDY MIGHT AFFECT RESEARCH, PRACTICE OR POLICY

- ⇒ This pilot study demonstrated the potential feasibility of an electromagnet as a portable alternative to fluoroscopy for accurate and efficient placement of endovascular devices for rapid hemorrhage control.
- ⇒ Whereas additional refinement, regulatory approval, and human clinical trials are required prior to use of this technology, this proof-of-concept study shows that magnetic sensors may represent a potential alternative to fluoroscopy in emergent settings.

for repair is problematic in the austere environment. Resuscitative Balloon Occlusion of the Aorta (REBOA) was adopted as an endovascular solution to this problem,<sup>2–4</sup> yet poses limitations related to ischemic complications, particularly when the balloon is placed proximally.<sup>5</sup> A retrievable Rescue stent graft was previously shown to provide temporary hemorrhage control and preserve distal perfusion.<sup>6,7</sup> However, a serious limitation of any endovascular technology is the need for imaging to facilitate accurate positioning relative to major vascular branches.<sup>8</sup>

© Author(s) (or their employer(s)) 2023. Re-use permitted under CC BY-NC. No commercial re-use. See rights and permissions. Published by BMJ.

**To cite:** Kenawy DM, Zhang Y, Elsisy M, et al. *Trauma Surg Acute Care Open* 2023;**8**:e001220.

Fluoroscopy has remained a gold standard for placement of endovascular devices, though in the setting of emergent endovascular hemorrhage damage control, there remain substantial logistical barriers. In most situations, it would be impossible to mobilize heavy fluoroscopic units prior to patient exsanguination, especially in the austere environment, and further magnified by the need for lead personal protective gowns and expertise with angiography for permanent endovascular repair. In addition, fluoroscopy is a distraction to other simultaneous activities that must occur when a patient is actively dying, such as airway placement and craniotomy, as examples. Ultimately, the incredibly short window for damage control of exsanguinating hemorrhage is incompatible with the logistics of fluoroscopy. An alternative approach would need to offer ease of use, portability, and freedom from environmental noise expected in the chaos of a military battlefield or a regional hospital after a civilian active shooter event.

Several methods for fluoroscopy-free positioning of endovascular devices in emergencies have been explored, but with limited capabilities.<sup>9–13</sup> Radiofrequency (RF) approaches have been explored in the literature, such as those used in domestic pet identification and retained surgical sponge detection.<sup>14 15</sup> Although this approach was well suited to relay information or “present/not present,” respectively, RF was not effective for accurate distance resolution and was too sensitive to environmental noise to be a viable alternative to the time-tested accuracy of fluoroscopic imaging. Conversely, electromagnets offer numerous advantages in detection. Magnetic field strength increases according to the Biot-Savart law as a sensor approaches the electromagnet, electromagnets are portable, and most importantly, the ability to cycle the electromagnet on and off allows one to sample and account for environmental noise, essentially a “noise cancelling” effect.<sup>16</sup>

The objective of this study was to analyze whether an intravascular magnetic sensor could provide comparable accuracy to the gold standard of fluoroscopy when positioning relative to an electromagnetic target over an anatomic landmark previously defined as a reference for vascular branches.<sup>17</sup> As such, the sensor would be passed within the vessel and constantly using the magnetic field strength to analyze the distance from the electromagnetic target, with the latter being positioned over a palpable anatomic landmark that can be used to predict where key vascular branches are located. Based on the results of a prior human vascular morphometry study,<sup>17</sup> the xiphoid is a palpable reference point for the location of visceral vessels. As a result, for the purposes of this study, an electromagnet was placed on the xiphoid as a “target” for the magnetic sensor. The sensor would then provide visual feedback on the screen to convey the distance between the sensor and the target in centimeters. It was important to model extreme environmental and physiologic conditions seen expected in austere environments, and this device was tested with the presence of ferrous metallic shrapnel and vibration, as well as tachycardia/hypertension and hypotension. We hypothesized that the sensor would be able to localize stent grafts within 1 cm of accuracy ( $\pm 0.5$  cm either direction from the target) regardless of environmental or physiologic conditions.

## METHODS

### Magnetic sensors

Two magnetic sensor prototypes were created. The magnetic sensor alone (MSA) consisted of a magnetic sensor secured to the distal end of a 0.035” Lunderquist guidewire (Cook Medical,

Bloomington, Indiana, USA). The magnetic sensor with integrated stent (MSIS) was intended to simulate the magnetic sensor integrated with a nitinol Rescue stent design as a model of the ultimate clinical use of this positioning system. Details of the sensor design and detection algorithm are detailed previously.<sup>16</sup> Briefly an electromagnet (BDE-3020–12, BUNTING, Newton, Kansas, USA) with a DC power supply (SE-350–24, MORNSUN, Doylestown, Pennsylvania, USA) was connected to a Raspberry Pi (Raspberry Pi 4 Model B, Cambridge, England) and used a relay to cycle the electromagnetic field (EMF) at 0.04 seconds to 0.08 seconds. A magnetometer (MMC5603NJ, MEMSIC, Tianjin, China) and accelerometer (MXC400xXC, MEMSIC) installed on the stent were also connected to the Raspberry Pi to measure the EMF and position in space, respectively. The sensor further contained radiopaque markers to allow co-localization fluoroscopically. The final size of the sensor was 30 mm long  $\times$  1.8 mm wide, which was compatible with catheter-based delivery.

### Porcine model

The ARRIVE (Animal Research: Reporting of *In Vivo* Experiments) guidelines 2.0 were used to develop this porcine model. Three female Yorkshire pigs ( $79 \pm 10$  kg) were placed under general endotracheal anesthesia. As previously described in the literature, heparin was given at a dose of 100 U/kg in light of the prothrombotic tendencies of the porcine model.<sup>6</sup> ECG and a femoral arterial line were used for monitoring of heart rate and blood pressure throughout the course of each experiment.

### In vivo evaluation of the magnetic sensor

An electromagnet was placed posterior to the animals at the level of the xiphoid process (a palpable landmark reference for visceral vessels).<sup>17</sup> The posterior location was chosen as a straighter segment, given the otherwise high arched anterior chest in the pig model at risk for parallax effect. In this setting parallax error occurs when the magnet and sensor appear aligned fluoroscopically, but in fact the angulation of the magnet would cause the magnetic field to be directed above the target and provide false readings. Glow N’ Tell Tape (LeMaitre, Burlington, Massachusetts, USA) was positioned with 0 cm at the xiphoid target.

A 10 French sheath was then introduced into the aorta for delivery of the MSA or MSIS (figure 1). The Raspberry Pi system provided visual feedback on a monitor of the distance between the sensor and the electromagnetic target. The external electromagnet was program cycled on and off, allowing a continuous calibration of outside electromagnetic noise. After magnetic sensor positioning at the level of the xiphoid (0 cm), 4 cm caudal to the xiphoid (+4 cm), or 12 cm caudal (+12 cm), fluoroscopy was used to obtain true position measurements of the sensor as compared with the magnet target. Measurements of the magnetic sensor and confirmatory fluoroscopic images were obtained at each location when the sensor was at 0 cm, +4 cm, and +12 cm ( $n=9$  per position and condition). The “true” fluoroscopic location as read from the Glow N’ Tell was then compared with the magnetic sensor location to analyze the degree of accuracy. Figure 2 demonstrates the position of the MSA and MSIS in an oblique view, and figure 3 demonstrates a lateral view with the electromagnet posterior to the aorta, at the level of the xiphoid process.

### Extreme conditions testing

Five different conditions were used to simulate extreme environmental and physiologic conditions encountered in patients with

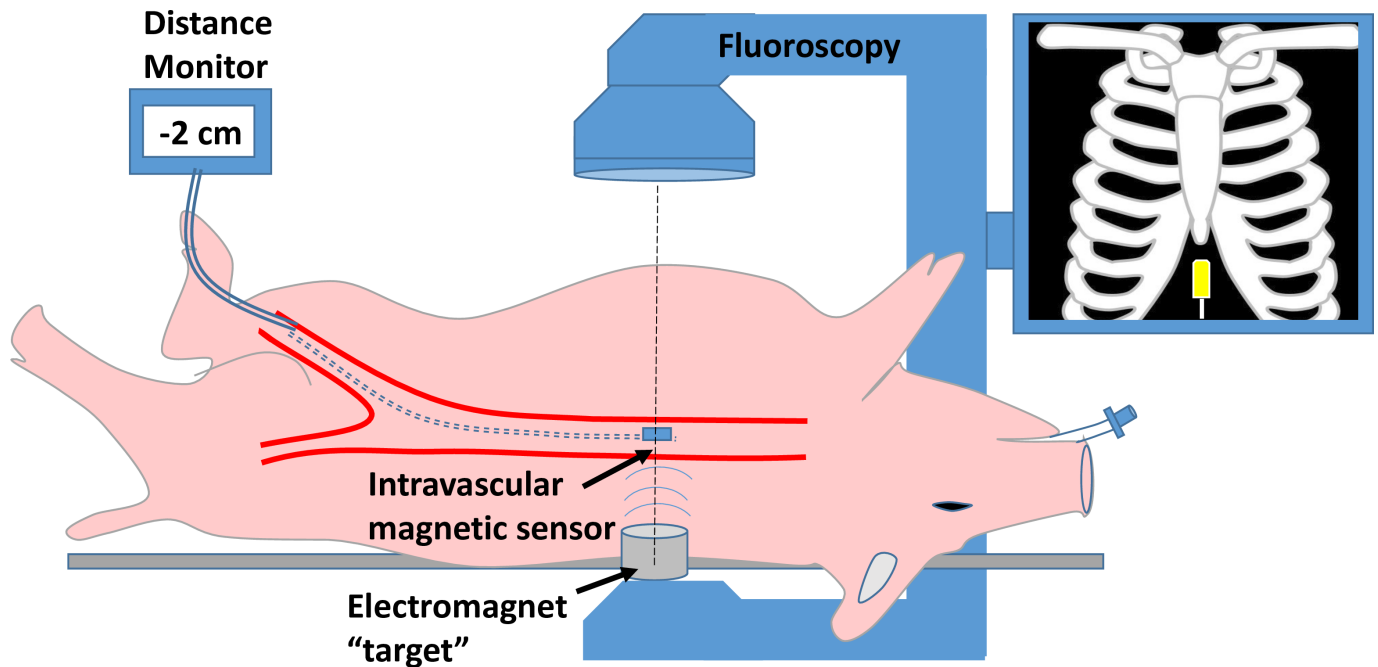


**Figure 1** Testing of a magnetic positioning sensor. A magnetic sensor placed from the groin, detects an electromagnet placed on the xiphoid. As the sensor approaches the “target” the distance is read on a monitor and validated with the true fluoroscopic location.

exsanguinating traumatic injuries and the effect on the MSA accuracy. These conditions included the following:

**Control:** Sensors were tested under hemodynamically normal conditions.

**Metal:** A large (0.5 kg) ferrous object (metal wrench) was placed adjacent to the magnet (inside the animal, within 10 cm of the sensor) to simulate shrapnel.

**Vibration:** Vibration at 40 Hz was used to simulate transportation within a battlefield environment, in particular a helicopter.

**Tachycardia/hypertension:** Animals were given 1 mg epinephrine injections for a minimum mean arterial pressure (MAP) goal of 120 and minimum heart rate of 150. Epinephrine was re-dosed as needed to maintain goal hemodynamic parameters.

**Hemorrhage (hypotensive):** Animals underwent hemorrhage until a maximum MAP of 30 was achieved.

After testing of the MSA, the MSIS was developed to assess our magnetic sensor design more rigorously under physiologic extremes, evaluating for the potential interference of a nitinol stent structure. As we had already confirmed that simulated shrapnel and vibration did not impact the MSA alone, the MSIS was only tested under conditions of control, tachycardia/hypertension, and hemorrhage conditions.

### Temperature testing

The electromagnet used in this study was noted to become warmer with prolonged use. To assess the effects of temperature on accuracy of readings, measurements were obtained ex vivo with the electromagnet at temperatures ranging from 22°C to

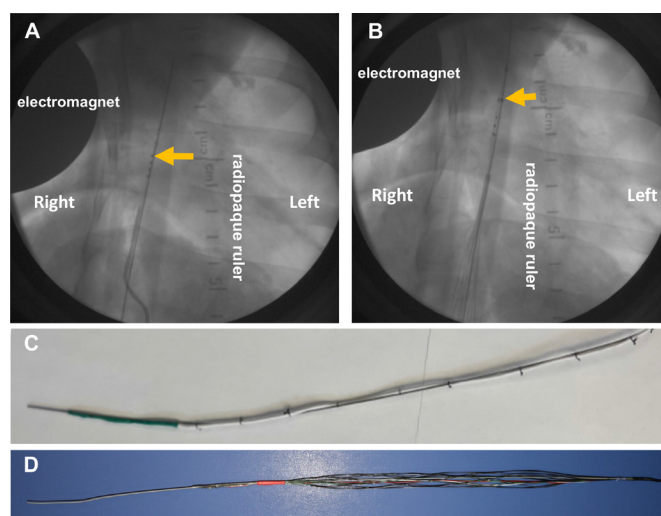


**Figure 2** Fluoroscopic images of (A) magnetic sensor alone (MSA) and (B) magnetic sensor with integrated stent (MSIS). Images of the (C) MSA and (D) MSIS.

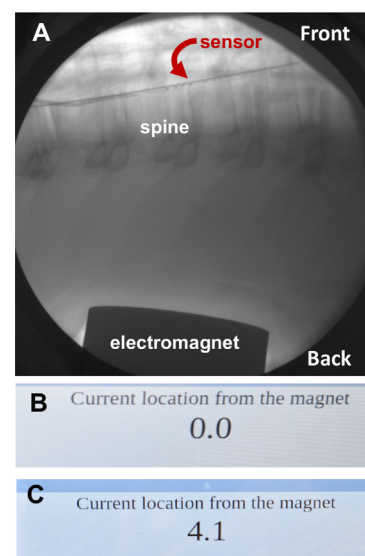


**Figure 3** (A) Lateral fluoroscopic view of sensor demonstrating electromagnet posterior to the spine. Visual readout for (B) 0 cm and (C) 4 cm are shown.

**Table 1** Hemodynamics of magnetic sensor alone (MSA) and magnetic sensor with integrated stent (MSIS) by condition

Sensor	Condition	Heart Rate (beats/min)	Systolic Blood Pressure (mm Hg)	Diastolic Blood Pressure (mm Hg)	MAP (mm Hg)
MSA	Control	83.4±14.3	64.0±7.6	46.5±5.9	52.3±6.2
	Metal	90.5±5.9	65.1±5.4	47.7±4.5	53.5±4.3
	Vibration	92.8±6.0	63.9±6.9	44.4±4.7	50.9±5.4
	Epinephrine	184.2±54.2	198±21	128±18	151±19
	Hemorrhage	129.9±23.6	39.2±3.7	30.4±5.3	33.3±4.6
MSIS	Control	110.2±8.4	52.6±5.6	42.4±2.3	45.8±2.8
	Epinephrine	169.1±24.1	183±29	110±26	135±27
	Hemorrhage	165.0±9.0	9.1±3.1	7.6±2.4	8.1±2.3

Shown are the means with SD.

MAP, mean arterial pressure; MSA, magnetic sensor alone; MSIS, magnetic sensor with integrated stent.

37°C. Measurements were again taken using the MSIS at 0 cm away from (ie, directly above) the electromagnet, with the sensor placed at a consistent height above the electromagnet. A total of 36 measurements were taken across this range of temperatures. Readings were confirmed using a ruler.

### Statistical analysis

Continuous variables were summarized as means and 95% CIs. Mean differences in true versus magnetic sensor readings were estimated using general linear statistical models including the difference as the dependent variable and the sensor type (MSA and MSIS), condition, and their interaction as independent variables. Hypothesis testing was conducted to test whether the estimated mean differences differed from 0, and to test differences in condition with the control condition within each sensor prototype. Hypothesis testing was conducted at a 5% type I error rate. Box plots were used to graphically display differences in true versus magnetic sensor readings by condition at different positions. Statistical analysis was conducted using SAS V.9.4 (SAS Institute, Cary, North Carolina, USA).

### RESULTS

Both the sensor alone (MSA) and in conjunction with a retrievable stent (MSIS) were compatible with a sheath-based intravascular delivery. Although the system was designed to read out distance on approach to the target from below, it also would read distance if the target was overshoot so the sensor could be withdrawn back to the 0 cm point. The system provided real-time feedback on the distance from the sensor to the target in centimeters on a portable monitor. Hemorrhage and epinephrine successfully reproduced tachycardia with hypotension and tachycardia, respectively, as shown in the physiologic data of [Table 1](#). [Figure 4](#) demonstrates the mean differences at each position and condition tested for both sensors. Using the MSA, we demonstrated that the mean difference was within our target of  $\pm 0.5$  cm for all experimental conditions at distances of 0 cm and +4 cm ([Table 2](#)). Despite the mean of  $\pm 0.5$  cm, a few conditions of the MSA (eg, at 0 cm: control: 0.41 (0.17, 0.66); epinephrine: 0.40 (0.16, 0.65); hemorrhage: 0.26 (0.01, 0.51)) were outside the  $\pm 0.5$  cm range. Despite being statistically significant, when positioned at 0 cm and +4 cm, only a few individual MSA readings approached a centimeter from the “true value” (eg, MSA at 0 cm control demonstrated a difference of 0.99 cm). We further identified that the MSA was less reliable at +12 cm from the target with mean difference outside our target error of under 0.5 cm in all but the control condition. Similarly, when using the control condition as our reference, we found that MSA readings at 0 cm and +4 cm were consistently within our accepted difference of  $\pm 0.5$  cm, with no significant difference in the mean differences for these conditions.

With the MSIS, all mean differences at 0 cm and +4 cm except for one (hemorrhage at position 0 cm demonstrated a mean difference of 0.51 cm) were within our target of  $\pm 0.5$  cm ([table 2](#)). Although mean differences under conditions of epinephrine and hemorrhage technically yielded statistical significance, the mean differences remained clinically insignificant, well within our target mean of  $\pm 0.5$  cm. Using control as our reference point, there was no significant difference in experimental conditions at 0 cm and +4 cm. Once again, we found a trend towards increasing inaccuracy at the +12 cm position, with mean differences outside our target of  $\pm 0.5$  cm.

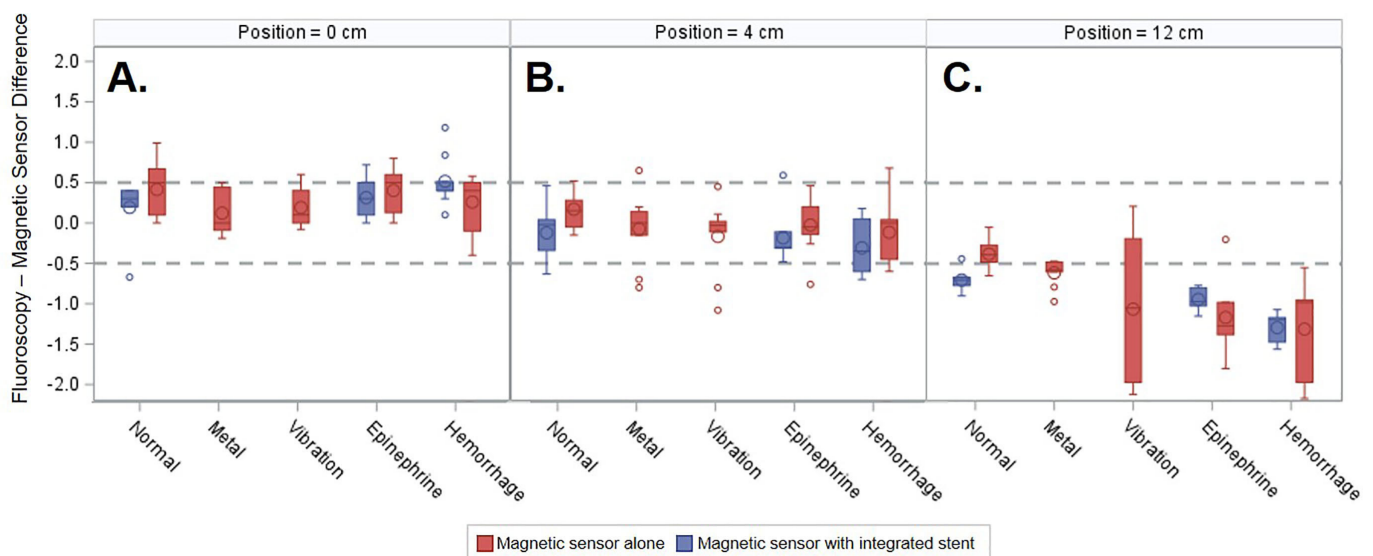


**Figure 4** Box plots demonstrating differences in readings between fluoroscopy and magnetic sensor at distances of (A) 0 cm, (B) +4 cm, and (C) +12 cm. Median is represented by the inner line, mean is represented by the inner circle, IQR is represented by the length of each box, and 1.5 times the IQR is represented by the whiskers.

**Table 2** Difference in position of fluoroscopy and magnetic sensor alone (MSA) and magnetic sensor with integrated stent (MSIS) readings separated by condition, and position, with positive readings indicating a position caudal to the magnet

Sensor	Position (cm)	Condition	Fluoroscopy—Magnet (cm) mean (95% CI)	P value (difference from fluoroscopy)	Difference from "control" (cm) mean (95% CI)	P value (difference from "control")
MSA	0	Control	0.41 (0.17, 0.66)	0.0011*	Reference	–
	0	Epinephrine	0.40 (0.16, 0.65)	0.0015*	–0.01 (-0.36, 0.34)	0.945
	0	Hemorrhage	0.26 (0.01, 0.51)	0.0398*	–0.16 (-0.50, 0.19)	0.3804
	0	Metal	0.12 (-0.12, 0.37)	0.3298	–0.29 (-0.64, 0.06)	0.1002
	0	Vibration	0.19 (-0.06, 0.44)	0.1283	–0.22 (-0.57, 0.13)	0.2084
	4	Control	0.17 (-0.08, 0.42)	0.1758	Reference	–
	4	Epinephrine	–0.03 (-0.27, 0.22)	0.8384	–0.20 (-0.54, 0.15)	0.2704
	4	Hemorrhage	–0.12 (-0.36, 0.13)	0.3568	–0.29 (-0.63, 0.06)	0.1082
	4	Metal	–0.07 (-0.32, 0.17)	0.5584	–0.24 (-0.59, 0.11)	0.1706
	4	Vibration	–0.17 (-0.41, 0.08)	0.1844	–0.34 (-0.69, 0.01)	0.0586
	12	Control	–0.38 (-0.63, to 0.13)	0.0026*	Reference	–
	12	Epinephrine	–1.17 (-1.41, to 0.92)	<0.0001*	–0.79 (-1.13, to 0.44)	<0.0001*
12	Hemorrhage	–1.31 (-1.56, to 1.06)	<0.0001*	–0.93 (-1.28, to 0.58)	<0.0001*	
12	Metal	–0.61 (-0.86, to 0.37)	<0.0001*	–0.23 (-0.58, 0.12)	0.1888	
12	Vibration	–1.06 (-1.31, to 0.82)	<0.0001*	–0.68 (-1.03, to 0.33)	0.0002*	
MSIS	0	Control	0.19 (-0.05, 0.44)	0.1261	Reference	–
	0	Epinephrine	0.31 (0.07, 0.56)	0.0131*	0.12 (-0.23, 0.47)	0.4945
	0	Hemorrhage	0.51 (0.27, 0.76)	<0.0001*	0.32 (-0.03, 0.67)	0.0701
	4	Control	–0.12 (-0.37, 0.12)	0.3298	Reference	–
	4	Epinephrine	–0.19 (-0.43, 0.06)	0.1397	–0.06 (-0.41, 0.29)	0.7208
	4	Hemorrhage	–0.31 (-0.55, to 0.06)	0.0148*	–0.19 (-0.53, 0.16)	0.2956
	12	Control	–0.70 (-0.95, to 0.46)	<0.0001*	Reference	–
	12	Epinephrine	–0.94 (-1.19, to 0.70)	<0.0001*	–0.24 (-0.59, 0.11)	0.1745
	12	Hemorrhage	–1.29 (-1.54, to 1.05)	<0.0001*	–0.59 (-0.94, to 0.24)	0.001*

Significant values of p marked with an asterisk (\*).

MSA, magnetic sensor alone; MSIS, magnetic sensor with integrated stent.

Ex vivo testing of the MSIS with the electromagnet over a range of working temperatures was performed at 0 cm to control for any variability in position and furthermore is the single most important location for device positioning. Only 4 of the 36 MSIS readings were non-zero, with a mean difference in the MSIS and true readings of  $-0.1$  cm (95%CI  $-0.21$  to  $0.01$ ,  $p=0.063$ ), indicating no significant difference in the mean difference in true versus sensor readings taken as the electromagnet temperature ranged from  $22^{\circ}\text{C}$  to  $37^{\circ}\text{C}$ .

## DISCUSSION

Rapid hemorrhage control is the top priority in NCTH, and yet current treatment modalities are limited. To address some of these concerns, it has previously been demonstrated that a novel retrievable Rescue stent graft can provide rapid hemorrhage control and improved survival compared with REBOA.<sup>6</sup> A vascular morphometry study later detailed an algorithm not only for patient triage to presized and retrievable damage control stent grafts based on height and gender, but also the critical relationship of major visceral aortic branches to palpable bony landmarks.<sup>17</sup> Numerous efforts have been made to address the issue of placement of endovascular NCTH control in the austere or emergency environment. Methods using standardized positions,<sup>10</sup> RF identification,<sup>9 14</sup> and even magnetic sensors<sup>12</sup> have been explored. However, the aforementioned vascular morphometry study suggests that variability of aortic lengths can complicate device positioning as premeasured metrics can be impacted by body size.<sup>17</sup> This morphometric diversity demands a method to track the intravascular device to a target. Although

fluoroscopy is a foundation of accurate elective endovascular interventions, the bulky nature and inherent radiation risks to bystanders in an emergency are impractical for the logistics of exsanguinating hemorrhage.

Instead, we investigated a magnetic sensor approach for emergent endovascular device placement. Rezende-Neto *et al*<sup>12</sup> proposed a similar magnetically trackable positioning system for the REBOA, though it was limited by the fact that the positioning system provided only auditory and visual feedback rather than precise distance measurements to localize the distance of the sensor from the magnet. Moreover, their device, although tested in a hemorrhagic porcine model, was not validated under the environmental “noise” conditions as with this study.<sup>12</sup>

A particular advantage of our approach, contrasting to the use of a permanent magnet in the Rezende-Neto study, is our use of an electromagnet. As the electromagnet can be cycled “on” and “off,” baseline EMFs can be sampled by the magnetic sensor and accounted for, similar to the “white balance” calibration of a photographic camera. This offers a particular “noise cancelling” advantage for the austere situation where environmental noise such as metallic shrapnel, vibration during transportation, or electromagnetic interference from nearby medical devices may negatively impact accuracy. We reasoned such self-calibration may also account for changing physiologic parameters such as extremes in heart rate and blood pressure. Finally, the rapid cycling of the magnet at 0.04 seconds to 0.08 seconds allows for rapid assessment of location for the magnetic sensor during intravascular placement.<sup>16</sup>

A difference of  $\pm 0.5$  cm in the fluoroscopy versus magnetic sensor readings was analyzed to be clinically acceptable. This device is envisioned for potential use with a retrievable damage control stent graft, either as a single tier stent graft<sup>14</sup> or three-tier Rescue stent graft, as previously reported,<sup>6</sup> which consists of a proximal and distal covered zone to control injuries to the descending thoracic and infrarenal abdominal aorta, respectively, whereas a bare-metal middle tier facilitates continued perfusion to the visceral branches of the abdominal aorta. Proper alignment of the bare metal section is crucial to prevent organ ischemia.

The magnetic sensor was least accurate further away (+12 cm) from the target and more accurate as it approached the target, such that at 0 cm and +4 cm; the mean difference in accuracy for both sensors was within  $\pm 0.5$  cm, except for one condition when MSIS with hemorrhage revealed a mean of 0.51 cm, a mere millimeter over our target. This value is well within the tolerable margin of error highlighted in the aforementioned human morphometry study.<sup>17</sup> The reduced accuracy at +12 cm is of less importance clinically since it does not define final device placement. Rather the accuracy improves once the sensor makes the final approach on the actual target; as a result the accuracy at +12 cm is probably not significant to the clinical utility.

The sensor, both alone and integrated with the retrievable stent, showed no clinically significant difference under any experimental condition when compared with “control” conditions at 0 cm and +4 cm (table 2), indicating improvement in accuracy with increasing proximity to the target.

The magnetic sensor was maintained under conditions that might otherwise seem disruptive to sensors, including increased aortic impulse (tachycardia and hypertension). Although we did not specifically examine under conditions of bradycardia or asystole, these represent low impulse states and are less likely to impact magnetic sensor performance. Future investigations should include formal evaluation under all physiologic and environmental conditions expected in an environment where torso hemorrhage occurs.

Our study was particularly reassuring in the presence of ferrous shrapnel, which might intuitively seem prohibitive for a magnetic positioning system. This latter finding highlights an especially important feature of this system. By cycling the electromagnet target on and off, the system is continuously sampling the environment, which allows accuracy in the face of electromagnetic noise. The frequent sampling of the environment at 0.04 seconds to 0.08 seconds ensures the system is accounting for dynamic changes in environmental noise and rapid feedback of position to the care provider.

Notably, in this study, the electromagnet was placed posterior to the animal, aligned with the xiphoid, a surrogate for major vascular branches of the aorta. Arguably the magnet could also be placed anterior to the xiphoid, and we found the sensor to be effective at up to 26 cm from the aorta in this position. The reason we elected not to use a front-placed magnet was because the deep chested porcine model created parallax effect with the magnet angled cephalad, thereby creating an error between the “true” and magnetic sensor position. Posterior placement perpendicular to the sensor path therefore produced greater consistency in the experimental design. Ultimately, parallax effect may be a limitation of this device in humans, with the back potentially providing a more consistent surface for magnet placement to avoid the angle deviation that accompanies different types of body habitus at the xiphoid (eg, scaphoid vs obese abdomen). Although our study demonstrated good accuracy within a consistently sized porcine model with a depth

averaging up to 10 cm from skin to aorta from a magnet placed on the back, future examination across a wide spectrum of body habitus types in humans will be an important validation. Drift is the tendency of a sensor to adversely bias accuracy with the passing of time or changes in temperature, for instance. Importantly, our study revealed no significant loss of accuracy over either condition, although temperature extremes such as a desert or arctic environment certainly would need evaluation prior to clinical use in such environments. Although we had some initial concerns that the accuracy of the sensor might decrease due to rising magnet temperature with prolonged use in our in vivo model, ex vivo testing confirmed there was no significant relationship between rising difference in true and sensor readings as temperature increased. Nevertheless, future iterations of this system should include electromagnets with optimized wire gauge to reduce heat generation. It is also noteworthy that although passage of endovascular devices without fluoroscopy would seem treacherous due to aneurysms and arterial occlusions, in fact most civilian and battlefield NCTH occur in a young demographic free of these barriers to intravascular device passage. Moreover, these small risks may be justified given the otherwise certain death from rapid exsanguination. The use of a 10 French sheath in this study was largely related to the large gauge wires to which the otherwise small sensor was attached. Future iterations will certainly reduce the wire gauge and are expected to reduce the delivery profile further, as well as produce a more portable delivery system (eg, battery powered electromagnet to eliminate the need for DC power supply). Moreover, while this study examined the magnetic sensor integrated with a retrievable stent graft, the technology certainly should be compatible with other intravascular hemorrhage control approaches. Although this study depicts a porcine model with depths comparable to the human condition, the model was relatively consistent contrasting to a diverse body type of the human population. Rigorous testing in a human cadaver model with varied degree of adipose tissue and size will be critical prior to human use. Moreover, although several categories of simulated environmental noise were examined, testing of all implants both metallic and those generating EMFs will be equally important in the next phases of this technology.

In conclusion, this pilot study demonstrated that a magnetic sensor and electromagnet can be used in conjunction with fixed palpable anatomic landmarks to accurately localize endovascular hemorrhage control devices in emergency settings where use of fluoroscopy would otherwise be prohibitive. Importantly, this was a pilot study of a novel approach for device placement and will require further refinement, validation, regulatory approval, and human clinical trials before it can be considered for human clinical care.

**Acknowledgements** The authors thank Marlene I. Garcia-Neuer, MD, MSc for her assistance in data collection during this study.

**Contributors** DMK and BWT were involved in all aspects of the study, including literature search, study design, data collection, analysis, and interpretation, development of the article, and critical revision. YZ, ME, YC, and WCC were involved in study design and critical revision. MA-R was involved in data analysis and critical revision. BWT is the guarantor for this manuscript.

**Funding** This work was supported by the Assistant Secretary of Defense for Health Affairs, through the Defense Medical Research and Development Program under Award No. W81XWH-16-2-0062 (BWT). Opinions, interpretations, conclusions, and recommendations are those of the authors and are not necessarily endorsed by the Department of Defense. This research was also supported by the National Institutes of Health under the Ruth L. Kirschstein National Research Service Award, from the National Institute of Allergy and Infectious Diseases of the National Institutes of Health under Award Number NIH T32AI106704 (DMK) and the National Center for Advancing Translational Sciences of the National Institutes of Health under Grant

Number UL1TR002733 (MA-R). The content is solely the responsibility of the authors and does not necessarily represent the official views the National Institutes of Health.

**Competing interests** An invention disclosure was submitted for the device detailed in this article.

**Patient consent for publication** Not applicable.

**Ethics approval** Institutional Animal Care and Use Committee (2020A00000087)

**Provenance and peer review** Not commissioned; externally peer reviewed.

**Data availability statement** Data are available upon reasonable request. All data are available upon reasonable request to the corresponding author of this article.

**Open access** This is an open access article distributed in accordance with the Creative Commons Attribution Non Commercial (CC BY-NC 4.0) license, which permits others to distribute, remix, adapt, build upon this work non-commercially, and license their derivative works on different terms, provided the original work is properly cited, appropriate credit is given, any changes made indicated, and the use is non-commercial. See: <http://creativecommons.org/licenses/by-nc/4.0/>.

#### ORCID iDs

Dahlia M Kenawy <http://orcid.org/0000-0002-6096-9978>

Bryan W Tillman <http://orcid.org/0000-0001-5769-0012>

#### REFERENCES

- Morrison JJ, Rasmussen TE. Noncompressible torso hemorrhage: a review with contemporary definitions and management strategies. *Surg Clin North Am* 2012;92:843–58.
- Russo RM, Neff LP, Johnson MA, Williams TK. Emerging endovascular therapies for non-compressible torso hemorrhage. *Shock* 2016;46:12–9.
- Moore LJ, Brenner M, Kozar RA, Pasley J, Wade CE, Baraniuk MS, Scalea T, Holcomb JB. Implementation of resuscitative endovascular balloon occlusion of the aorta as an alternative to resuscitative thoracotomy for noncompressible truncal hemorrhage. *J Trauma Acute Care Surg* 2015;79:523–30.
- DuBose JJ, Scalea TM, Brenner M, Skiada D, Inaba K, Cannon J, Moore L, Holcomb J, Turay D, Arbabi CN, et al. The AAST prospective aortic occlusion for resuscitation in trauma and acute care surgery (AORTA) registry: data on contemporary utilization and outcomes of aortic occlusion and resuscitative balloon occlusion of the aorta (REBOA). *J Trauma Acute Care Surg* 2016;81:409–19.
- Long KN, Houston R, Watson JDB, Morrison JJ, Rasmussen TE, Propper BW, Arthurs ZM. Functional outcome after resuscitative endovascular balloon occlusion of the aorta of the proximal and distal thoracic aorta in a swine model of controlled hemorrhage. *Ann Vasc Surg* 2015;29:114–21.
- Go C, Elsisy M, Chun Y, Thirumala PD, Clark WW, Cho SK, Demetris AJ, Tillman BW. A three-tier rescue stent improves outcomes over balloon occlusion in a porcine model of noncompressible hemorrhage. *J Trauma Acute Care Surg* 2020;89:320–8.
- Go C, Chun YJ, Kuhn J, Chen Y, Cho SK, Clark WC, Tillman BW. Damage control of caval injuries in a porcine model using a retrievable rescue stent. *J Vasc Surg Venous Lymphat Disord* 2018;6:646–56.
- Olsen MH, Thonghong T, Søndergaard L, Møller K. Standardized distances for placement of REBOA in patients with aortic stenosis. *Sci Rep* 2020;10:13410.
- Wessels LE, Wallace JD, Bowie J, Butler WJ, Spalding C, Krzyzaniak M. Radiofrequency identification of the ER-REBOA: confirmation of placement without fluoroscopy. *Mil Med* 2019;184:e285–9.
- Pezy P, Flaris AN, Prat NJ, Cotton F, Lundberg PW, Caillot J-L, David J-S, Voiglio EJ. Fixed-distance model for balloon placement during fluoroscopy-free resuscitative endovascular balloon occlusion of the aorta in a civilian population. *JAMA Surg* 2017;152:351–8.
- Sokol KK, Black GE, Shawhan R, Marko ST, Eckert MJ, Tran NT, Starnes BW, Martin MJ. Efficacy of a novel fluoroscopy-free endovascular balloon device with pressure release capabilities in the setting of uncontrolled junctional hemorrhage. *J Trauma Acute Care Surg* 2016;80:907–14.
- Rezende-Neto JB, Ravi A, Semple M. Magnetically trackable resuscitative endovascular balloon occlusion of the aorta: a new non-image-guided technique for resuscitative endovascular balloon occlusion of the aorta. *J Trauma Acute Care Surg* 2020;88:e87–91.
- Scott DJ, Eliason JL, Villamaria C, Morrison JJ, Houston R 4th, Spencer JR, Rasmussen TE. A novel fluoroscopy-free, resuscitative endovascular aortic balloon occlusion system in a model of hemorrhagic shock. *J Trauma Acute Care Surg* 2013;75:122–8.
- Chun Y, Cho SK, Clark WC, Wagner WR, Gu X, Tevar AD, McEnaney RM, Tillman BW. A retrievable rescue stent graft and radiofrequency positioning for rapid control of noncompressible hemorrhage. *J Trauma Acute Care Surg* 2017;83:249–55.
- Rogers A, Jones E, Oleynikov D. Radio frequency identification (RFID) applied to surgical sponges. *Surg Endosc* 2007;21:1235–7.
- Zhang Y, Clark WW, Tillman B, Chun YJ, Liu S, Cho SK. A system to track stent location in the human body by fusing magnetometer and accelerometer measurements. *Sensors* 2023;23:4887.
- Go C, Fish L, Chun Y, Alarcon L, Tillman BW. The anchor point algorithm: a morphometric analysis of anatomic landmarks to guide placement of temporary aortic rescue stentgrafts for non-compressible torso hemorrhage. *J Trauma Acute Care Surg* 2022;93:488–95.